

Magnetic Resonance Imaging of Iron in Parkinson's Disease

Kazuo Abe* and Tachio Hikita

Department of Neurology, Osaka University Graduate School of Medicine D-4, 2-2 Yamadaoka, Suita, Osaka 565-0871, Japan

Abstract: The primary pathology of idiopathic Parkinson's disease (PD) is degeneration of the substantia nigra pars compacta. This leads to a reduction in striatal dopamine, which results in the cardinal symptoms of bradykinesia, tremor and rigidity. Increased iron content is consistently reported post-mortem in the substantia nigra of patients with PD and reactive microglia and its capacity to enhance production of toxic reactive oxygen radicals. This may suggest that iron-related oxidative stress may be an important component of the neurodegenerative process in such patients. Presently the mechanisms involved in the disturbances of iron metabolism in PD remain obscure, but evaluating iron contents in brain of PD may be important.

Evaluation of iron contents in brain has been possible only with post-mortem study, but advent of MRI techniques makes it possible to evaluate brain iron deposits *in vivo*. However, previous studies have been inconsistent with the findings compared with post-mortem investigations. This suggests that improved MRI techniques may be useful for assessing brain iron deposits with greater accuracy.

In this mini-review, we discussed investigations for assessing brain iron in PD.

Keywords: Magnetic resonance imaging (MRI), iron, parkinson's disease (PD), transverse relaxation time, spin echo (SE), gradient echo (GE).

INTRODUCTION

In his classic 1817 monograph "Essay on the Shaking Palsy," James Parkinson described the core clinical features of Parkinson's disease (PD)[1]. After about more than a century, the central pathological feature of PD was found to be degeneration of the substantia nigra pars compacta (SNpc) [2, 3]. This leads to a reduction in striatal dopamine, which results in the cardinal symptoms of bradykinesia, tremor and rigidity. Based on these researches, replenishment of striatal dopamine (DA) through the oral administration of the DA precursor levodopa (L-3, 4-dihydroxyphenylalanine) was started and alleviates most of these symptoms. Although the discovery of levodopa revolutionized the treatment of PD, we soon learned that after several years of treatment most patients develop undesirable symptoms such as dyskinesias and freezing which are difficult to control and significantly impair the quality of life. Thus, current research is directed toward developing neuroprotective drugs to halt or retard neuron degeneration in PD. In such situation, brain iron metabolism in PD has accumulated attention in relation to oxidative stress to the SNpc [4].

Increased iron content is consistently reported post-mortem in the SNpc of patients with PD [5, 6] and reactive microglia and its capacity to enhance production of toxic reactive oxygen radicals. This may suggest that iron-related oxidative stress may be an important component of the neurodegenerative process in such patients, although there

are controversy [4]. Presently the mechanisms involved in the disturbances of iron metabolism in PD remain obscure, but evaluating iron contents in brain of PD may be important.

EVALUATION OF BRAIN IRON BY MAGNETIC RESONANCE IMAGE (MRI)

General Aspects

Iron exists *in vivo* roughly in two different forms; heme and nonheme iron. Heme iron exists mainly as hemoglobin and myoglobin, and nonheme iron mainly as ferritin and hemosiderin bound to nonheme iron [5-10]. The relationship between iron metabolism and disease process in degenerative diseases in the central nervous system (CNS) has become clearer through such concepts as oxidative stress [4, 11]. In a postmortem study, Hallgren found nonheme iron deposits mainly in the basal ganglia, and an increase in iron deposits along with aging [5-7]. Nonheme iron deposits are more abundant in neurodegenerative disorders than in controls [12]. Thus, estimating iron deposits is critical for analyzing neurodegenerative process in these diseases.

Since local magnetic inhomogeneity reduces the transverse relaxation rate of MRI, the amount of iron deposits in tissue can be estimated by measuring this rate [13, 14]. On average, one-third of the brain iron content is stored in the form of the metalloprotein ferritin [5]. The form of iron is important because the effects of ferritin on MR imaging are different from those of other biologic forms of iron. All ferritins have 24 protein subunits arranged in 432 symmetry to give a hollow shell with an 80 Å diameter cavity capable of storing up to 4500 Fe_(III) atoms as an inorganic complex. Its ability to sequester the element gives ferritin the dual functions of iron detoxification and iron

*Address correspondence to this author at the Associate Professor, Department of Neurology, Osaka University Graduate School of Medicine D-4, 2-2 Yamadaoka, Suita, Osaka 565-0871, Japan; Tel/Fax: +81-6-6879-3571/+81-6-6879-3579; E-mail: abe@neuro.med.osaka-u.ac.jp

reserve. The T_2 effect of ferritin is much stronger than the T_1 effect [15-23].

Since iron accumulation affects the MR signal (particularly T_2), attempts have been made to monitor changes in iron deposits in patients with PD by using MR T_2 relaxometry [24, 26], a combination of T_2 - and T_2^* -weighted images [26], and the dependence on interecho timing of T_2 relaxometric sequences [27]. Imaging a pure sample placed in a homogeneous B_0 (where B_0 is the magnitude of the main static magnetic field) field, the following a 90° RF pulse, the free induction decay (FID) will decay away with time constant T_2 . If the field is not pure, spin in the different field losing phase coherence, and the FID decaying faster than if the sample were in a pure field. An inhomogeneous B_0 field therefore introduces additional dephasing, on top of that generated by the random thermal activity of the sample. The time constant that describes the decay of the FID in such circumstances is known as R_2^* and is given by the summation of the natural transverse relaxation rate R_2 ($R_2 = 1/T_2$) plus an additional relaxation term, R_2' ($R_2' = 1/T_2'$), such that

$$R_2^* = 1/T_2^* = R_2 + R_2' = 1/T_2 + 1/T_2' \quad (\text{Equation 1})$$

Note that T_2^* is contribute to by 'natural' T_2 process and also additional effects. The effects of inhomogeneous B_0 field can be eradicated by the use of a spin echo. However, again, it must be stressed that these effects are only eliminated at the peak of a spin echo train, the signal decays away more rapidly than that observed with pure T_2 relaxation (Fig. 1) [28, 29]. In other words, inhomogeneities of samples may be separated into global (R_2) and local (R_2') field inhomogeneities. Consequently, transverse magnetization of MRI is lost at an exponential rate R_2^* ($e^{R_2^*t}$). A 180° pulse can be used to refocus the phase of protons, causing them to recover transverse magnetization. The maximum intensity of the signal is limited by an exponential rate R_2 (e^{R_2t}).

Generally, R_2 is the irreversible contribution and R_2' is the reversible contribution to the 180° -pulse. The 180° -pulse is frequently used to correct local magnetic inhomogeneity.

A hypothesis has widely been accepted that the local magnetic inhomogeneity caused by iron is affected by R_2' but not by R_2 (Fig. 2) [26,28,30,31]. Ordidge measured R_2 , R_2' , and R_2^* using special sequence and concluded that R_2' was affected predominantly by iron deposits [26]. However, accumulating evidences have suggested that R_2 as well as R_2' was affected by iron deposits [20, 30-34]. Thus, it is possible to evaluate brain iron deposits *in vivo* using high-field strength spin-echo T_2 weighted MRI [35]. T_2 relaxation time is shortened in approximate proportion to regional iron content [33, 35] and appears as signal hypointensity in T_2 weighted MRI. Signal reduction is due to additional proton spin dephasing from iron-induced local field inhomogeneities. This additional dephasing is detected because radiofrequency refocusing cannot compensate for it. With advent of MR sequence techniques, it becomes a matter of controversy whether the local field inhomogeneity induced by iron deposits is affected only by R_2' or by both R_2 and R_2' [36-38].

Appropriate Pulse Sequences for Evaluation of Brain Iron in PD

To determine appropriate pulse sequences for evaluation of brain iron accumulation in neurological diseases including PD, many attempts have been going on [36-40].

Ma *et al.* introduced the GESFIDE (gradient echo sampling of free induction decay and echo) sequence, which can simultaneously obtain the reversible and irreversible contributions [40]. GESFIDE is basically a Hahn [41] spin echo (SE) sequence (90° - TE/2- 180° - TE/2, where TE is abbreviation of echo time), and it collects a series of gradient echoes every five millisecond from the spin excitation to the spin echo at TE=120ms. From the GESFIDE data, the two effective relative rates were separately obtained, R_2^*A (prior

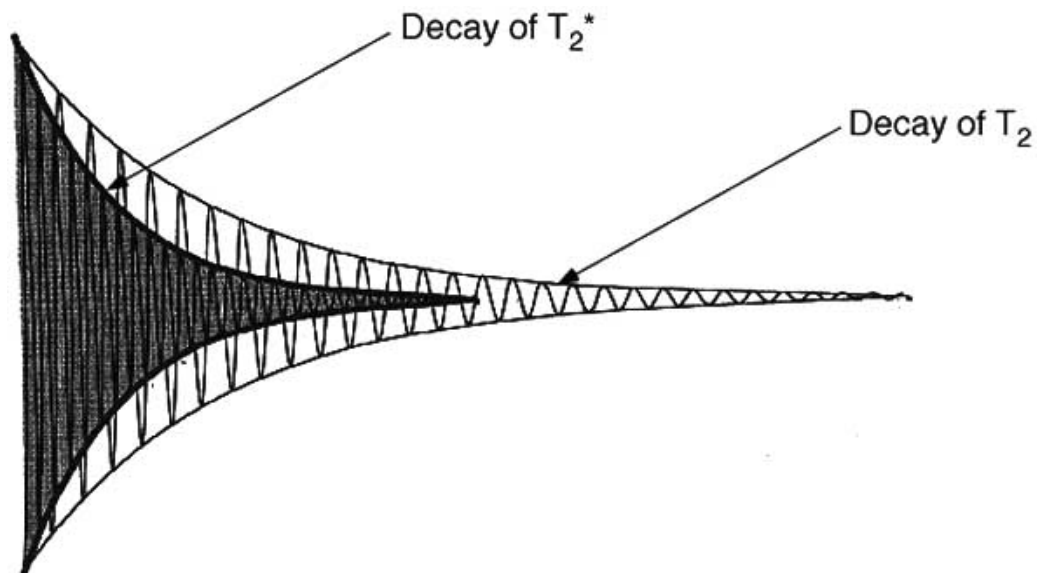


Fig. (1). Decay of T_2 and T_2^*

T_2^* signal decays away more rapidly than that observed with pure T_2 relaxation.

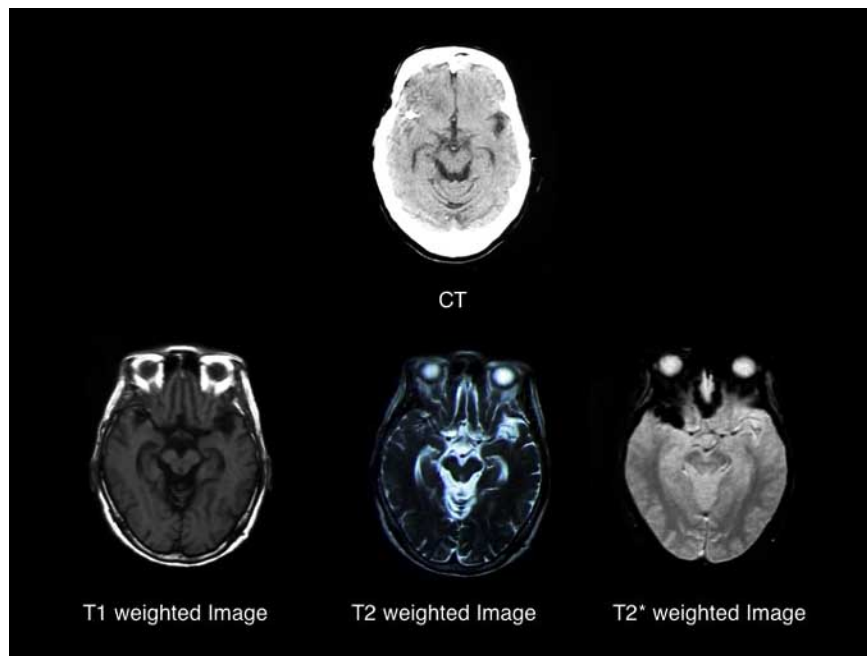


Fig. (2). Comparison of T₁-, T₂-, and T₂* weighted images

An aneurysm in the right middle cerebral artery was underwent a clipping operation. A clip showing high density in a CT image (upper) itself has weak magnetic effect. An old hematoma showed low intensity in a T₁ weighted image (lower left), vaguely high intensity in a T₂ weighted image (lower middle), and obviously low intensity in a T₂* weighted image (lower right).

to the 180°-pulse) and R_2^*B (after the 180°-pulse). R_2' was calculated as $1/2(R_2^*A - R_2^*B)$ and R_2 as $1/2(R_2^*A + R_2^*B)$. Graham *et al.* evaluated iron deposits in the basal ganglia in PD using a partially refocused interleaved multiple echo (PRIME) MRI sequence [14]. Their sequence yields both T₂* and T₂ information directly, from which T₂', a pure measure of local field inhomogeneity due to tissue iron content, can be obtained [14, 42]. Hikita *et al.* measured R_2 and R_2' of basal ganglia and frontal cortex by GE and by MSE in healthy volunteers and discussed advantage and disadvantage of both methods [30, 31]. According to their methods, representative R_2 maps based on the MSE (multiple spin echo) and GESFIDE sequences, and a representative R_2' maps based on GESFIDE are presented in (Fig. 3). In the R_2' map, high intensity lesions were enclosed in the rectangles A and B. Rectangle A is the borderline between the skull and the brain surface and rectangle B is a site above the skull base and paranasal sinus. Since these air-bone borderlines reproduced the magnetic susceptibility difference artifacts and represented as high intensity signals on R_2' map, identification of anatomical structures on this map may be difficult. In addition, they suggested that R_2 and R_2' have sensitivity to detect iron deposits, because R_2 and R_2' linearly increase with increments of iron deposits estimated by Hallgren's results [5, 30, 31]. Vymazal *et al.* studied correlation between the extent of iron deposits and transverse relaxation rates by using a 1.5 T MRI system, and described linear correlations between R_2 measuring by MSE and iron deposits [20]. Gelman *et al.* compared R_2 and R_2' measuring by GESFIDE using a 3T MRI system and reported linear

correlations between R_2 and R_2' measuring by GESFIDE and iron deposits [43].

To obtain clear correlations between transverse relaxation rate and iron deposits, higher magnetic strength is needed. However, higher magnetic strength may product local magnetic field disturbing homogeneity of basic magnetic field [28, 44]. Orididge considered that R_2' measured by a 3T MRI system showed the best correlation with the amount of iron deposits when magnetic field inhomogeneity was corrected [45]. If static magnetic field inhomogeneity is corrected, even a lower magnetic strength model such as 1.5T MR system produces satisfiable R_2' values. However, the correction of magnetic field inhomogeneity usually needs complex procedures and is not practical to evaluate iron deposits in the basal ganglia and SNpc where primary pathological processes are going on in PD. Consequently, to estimate iron deposits in these anatomical regions, R_2 measured by SE method may be reasonable. Although it is a matter of controversy whether brain iron deposits can be measured only by R_2' or by both R_2 and R_2' , some foregoing studies concluded that that R_2 had enough to detect the brain iron deposits [24, 30, 31, 33, 34]. There comes a question why some foregoing studies failed to find usefulness of R_2 . Weiskoff *et al.* found that R_2 and R_2' depended on the size of magnetic perturbers [46]. Protons around magnetic perturbers generate diffusion that prevents refocusing of spins after the 180° pulse and that are affected by the size of magnetic perturber. If sizes of magnetic perturbers are within a few micrometers, the diffusion effect increase and transverse relaxation rates of SE

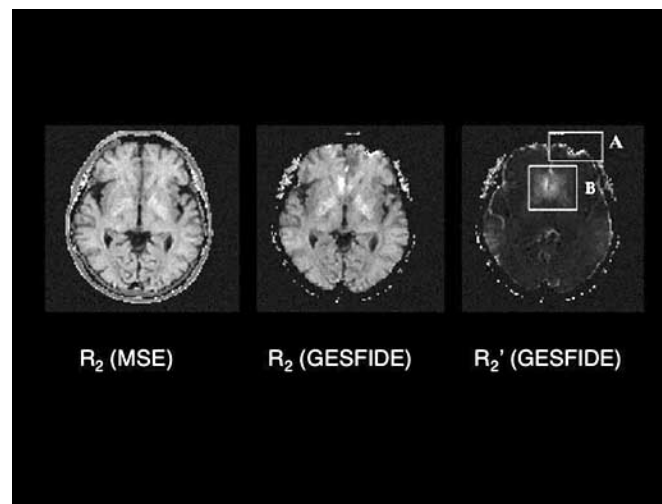


Fig. (3). R₂ and R₂' maps

R₂ and R₂' maps were arranged from the left to the right, a R₂ map based on MSE sequence (left), a R₂ map based on GESFIDE sequence (middle), and a R₂' map based on GESFIDE sequence (right).

and GE increase. But if they are larger enough to hundreds micrometers, the effect can be ignored [28, 46-48]. Since brain iron deposits mainly consisted with ferritin [5] that is only a few micrometers in diameters, the diffusion effect cannot be ignored. In such situation, SE has enough power to detect brain iron deposits in PD. In Figure 4, we demonstrated a representative R₂ and R₂' maps in a patient with PD that indicated R₂ measuring by MSE has enough power to demonstrate degenerative changes in basal ganglia without artifacts.

Main pathological processes in PD are going in the gray matter and we have mainly discussed iron deposits in the

gray matter. However, since the basal ganglia and brain stem have close connections to the cerebral cortices, neuronal pathways in the white matter may also be degenerated. Thus, we need to evaluate iron deposits in the white matter. To evaluate iron deposits in the white matter may be another problem. Foregoing studies, R₂ in the white matter was higher than it in the gray matter and failed to reflect iron deposits in the white matter [30, 31, 49]. This has been considered that components of water and lipid in the white matter are quite different from those in the gray matter [49]. Bartzokis *et al.* measured R₂ measured by a 0.5T system and measured also by a 1.5T system in brain tissues [49]. In their study, R₂ in the white matter decreased with aging, but it in

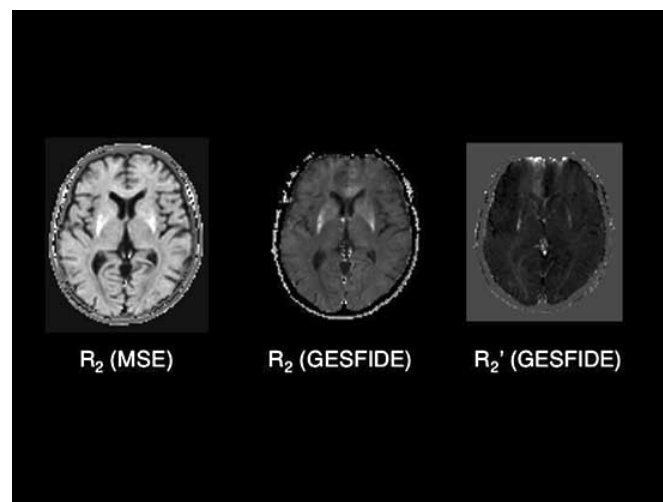


Fig. (4). R₂ and R₂' maps in a patient with Parkinson's disease

R₂ and R₂' maps were arranged from the left to the right, a R₂ map based on MSE sequence (left), a R₂ map based on GESFIDE sequence (middle), and a R₂' map based on GESFIDE sequence (right). R₂ measuring by MSE has enough power to demonstrate degenerative changes in basal ganglia without artifacts comparing with R₂ measuring by GESFIDE sequence and R₂' measuring by GESFIDE sequence.

the gray matter increased with aging. However, FDRI (field dependent R_2 increase) in the white matter and in the gray matter increased with aging. This suggests that the two different factors; one is the increment of R_2 due to iron deposits and another is the decrement of R_2 due to aging changes of brain tissue, may affect R_2 in the white matter. In gray matter of healthy volunteers, the increment factor overwhelms the decrement factor so that R_2 increases with aging. However, this may not be the case in degenerative diseases including PD where elevated tissue water substantially reduces R_2 and masks R_2 increment due to elevated brain iron deposits [50]. To compensate these, more sophisticated methods such as Bartzokis *et al.* described need to be adapted [51]. However, in PD, since we do not have enough observations to discuss iron deposits in the white matter, measuring iron deposits in the white matter is a future subject. In future investigations, in addition to above mentioned techniques, iron deposits in the white matter may be measured by relatively new techniques such as diffusion tensor imaging [52, 53] and mapping of cerebral hemoglobin contents [48, 54].

CONCLUSIONS

To evaluate brain iron deposits in PD, R_2 measured by GE may be most robust comparing with R_2 measured by SE or R_2' measured by GE. However, to evaluate iron deposits in the basal ganglia and SNpc of PD where primary pathological processes are going on, R_2 measured by SE may present reasonable values. To understanding degenerative process in PD, MRI evaluation of brain iron deposits in PD is important and presents chronological information that has never been given by pathological evaluations.

ACKNOWLEDGEMENTS

We are grateful Drs. Norihiko Fujita and Hisashi Tanaka for their useful advices for this manuscript.

REFERENCES

- [1] Parkinson J. Essay on the Shaking Palsy. Sherwood. Neely, and Jones, London, pp.1-66, 1817. (Arch Neurol Psychiat 1930; 23: 303-319.
- [2] Sano I, Gamo T, Takimoto Y, *et al.* Distribution of catechol compounds in human brain. Biochem Biophys Acta 1959; 32: 586-587.
- [3] Ehringer H, Hornikiewicz O. Verteilung von Noradrenalin und Dopamin (3-Hydroxytyramine) in Gehirn des Menschen und ihr Verhalten bei Erkrankungen des extrapyramidalen Systems. Wien Klin Wschr 1960; 38: 1236-1239.
- [4] Dauer W, Przedborski S. Parkinson's disease. Mechanism and Models. Neuron 2003; 39: 889-909.
- [5] Hallgren B, Sourander P. The effect of age on the nonhem iron in the human brain. J Neurochem. 1958; 3: 41-51.
- [6] Hill JM. The distribution of iron in the brain. In: Youdim MBH, Editor, Brain iron: neurochemical and behavioural aspects, Taylor and Francis, London 1988 pp. 1-24.
- [7] Griffiths PD, Crossman AR. Distribution of iron in the basal ganglia and neocortex in postmortem tissue in Parkinson's disease and Alzheimer's disease. Dementia 1993; 4: 61-65.
- [8] Bush AI. Metals and neuroscience. Current Opinion in Chemical Biology 2000; 4: 184-191.
- [9] Berg D, Gerlach M, Youdim MBH, *et al.* Brain iron pathways and their relevance to Parkinson's disease. Journal of Neurochemistry 2001; 79: 225-236.
- [10] Harrison PM, Arosio P. The ferritins: molecular properties, iron storage function and cellular regulation. Biochem Biophys Acta 1996; 1275: 161-203.
- [11] Gerlach M, Ben-Shachar D, Riederer P, Youdim MBH. Altered brain metabolism of iron as a cause of neurodegenerative disease? J Neurochem 1994; 63: 793-807.
- [12] Dexter DT, Jenner P, Schapira AHV, Marsden CD. Alterations in levels of iron, ferritin, and other trace metals in neurodegenerative disease affecting the basal ganglia. Ann Neurol 1992; 32: S94-S100.
- [13] Symms M, Jäger HR, Schmierer K, Youssry TA. A review of structural magnetic resonance neuroimaging. J Neurol Neurosurg and Psy 2004; 75: 1235-1244.
- [14] Graham JM, Paley MNJ, Grünewald RA, Hoggard N, Griffiths PD. Brain iron deposition in Parkinson's disease imaged using the PRIME magnetic resonance sequence. Brain 2000; 123: 2423-2431.
- [15] Bizzi A, Brooks RA, Brunetti A, *et al.* Role of iron and ferritin in MR imaging of the brain: a study in primates at different field strengths. Radiology 1990; 177: 59-65.
- [16] Vymazal J, Brooks RA, Zak O, *et al.* T1 and T2 of ferritin at different field strengths: effect on MRI. Magn Reson Med 1992; 27: 368-374.
- [17] Schenker C, Meier D, Wichmann P, Boesiger P, Alavanis A. Age distribution and iron dependency of the T2 relaxation time in the globus pallidus and putamen. Neuroradiology 1993; 35: 119-124.
- [18] Vymazal J, Hajek M, Patronas N, *et al.* The quantitative relation between T1- and T2-weighted MRI of normal gray matter and iron concentration. JMRI 1995; 5: 554-560.
- [19] Brooks RA, Vymazal J, Goldfarb R, Bulte JWM, Aisen P. Relaxometry and magnetometry of ferritin. Magn Reson Med 1998; 40: 227-235.
- [20] Vymazal J, Righini A, Brooks RA, *et al.* T1 and T2 in the Brain of Healthy Subjects, Patients with Parkinson Disease, and Patients with Multiple System Atrophy: Relation to Iron Content. Radiology 1999; 211: 489-495.
- [21] Ben-Schachar D, Eshel BA, Riederer P, Youdim MBH. Role of iron and iron chelation in dopaminergic-induced neurodegeneration: implication for Parkinson's disease. Ann Neurol 1992; 32(suppl): S105-S110.
- [22] Sian J, Dexter DT, Lees AJ, *et al.* Alterations in glutathione levels in Parkinson's disease and other neurodegenerative disorders affecting basal ganglia. Ann Neurol 1994; 36: 348-355.
- [23] Calne DB. The free radical hypothesis in idiopathic parkinsonism: evidence against it. Ann Neurol 1992; 32: 799-803.
- [24] Antonini A, Leenders KL, Meier D, *et al.* T2 relaxation time in patients with Parkinson's disease. Neurology 1993; 43: 697-700.
- [25] Bartzokis G, Cummings JL, Markham CH, *et al.* MRI evaluation of brain iron in earlier- and later-onset Parkinson's disease and normal subjects. Magn. Reson. Imaging 1999; 17: 213-222.
- [26] Ordidge RJ, Helpert JA, Knight RA, Deniau JC, Gorel JM. Assessment of relative brain iron concentrations using T2-weighted and T2*-weighted MRI at 3 Tesla. Magn Reson Med 1994; 32: 335-341.
- [27] Ye F, Allen PS, Martin WRW. Basal ganglia iron content in Parkinson's disease measured with magnetic resonance. Mov Disord 1996; 35: 119-124.
- [28] Boulby PA, Rugg-Gunn FJ. T2: the transverse relaxation time. In Quantitative MRI of the brain. Edited by Tofts P. Wiley & Sons Ltd., West Sussex 2003; pp143-201.
- [29] NessAiver M. All you really need to know about MRI physics. published by Moriel NessAiver PhD, 1997. (Japanese edition, Igaku-Shoin Ltd. Tokyo 1997.)
- [30] Hikita T, Abe K, Fujita N. Quantification of transverse relaxation rates for estimating iron deposits in the central nervous system. In Proceedings of the 12th scientific meeting and exhibition of International Society of Magnetic Resonance in Medicine p996, 2004.
- [31] Hikita T, Abe K, Sakoda S, *et al.* Determination of transverse relaxation rate for estimating iron deposits in the central nervous system. Neurosci Res (in press).
- [32] Antonini A, Leenders KL, Meier D, *et al.* T2 relaxation time in patients with Parkinson disease. Neurology 1993; 43: 697-700.
- [33] Bartzokis G, Aravagiri M, Oldendorf WH, Mintz J, Marder SR. Field Dependent Transverse Relaxation Rate Increase May Be a Specific Measure of Tissue Iron Stores. MRM 1993; 29: 459-464.
- [34] Georgiades CS, Itoh R, Golay X, van Zijl PCM, Melhem ER. MR imaging of the human brain at 1.5T: regional variations in

- transverse relaxation rates in the cerebral cortex. *AJNR* 2001; 22: 1732-1737.
- [35] Drayer BP, Burger P, Darwin R, *et al.* MRI of brain iron. *Am J Roentgenol* 1986; 147: 103-110.
- [36] Schenck JF. Magnetic resonance imaging of brain iron. *J Neurol Sci* 2003; 207: 99-102.
- [37] Ogg RJ, Langston JW, Haacke EM, Steen RG, Taylor JS. The correlation between phase shifts in gradient-echo MR images and regional brain iron concentration. *Magnetic Resonance Imaging* 1999; 17: 1141-1148.
- [38] Symms M, Jäger HR, Schmierer K, Yousry TA. A review of structural magnetic resonance neuroimaging. *J Neurol Neurosurg Psych* 2004; 75: 1235-1244.
- [39] Haque TL, Miki Y, Kanagaki M, *et al.* MR contrast of ferritin and hemosiderin in the brain: comparison among gradient-echo, conventional spin-echo and fast spin-echo sequences. *European Journal of Radiology* 2003; 48: 230-236.
- [40] Ma J, Wehrli FE. Method for image-based measurement of the transverse relaxation rate. *J Magn Reson B*. 1996; 111, 61-69.
- [41] Hahn EL. Spin echoes. *Phys Rev* 1950; 80: 580.
- [42] Miszkiel KA, Paley MN, Wilkinson ID, *et al.* The measurement of R2, R2*, and R2' in HIV-infected patients using the prime sequence as a measure of brain iron deposition. *Magn Reson Imaging* 1997; 15: 1113-9.
- [43] Gelman N, Gorell JM, Barker PB, *et al.* MR imaging of human brain at 3.0T : preliminary report on transverse relaxation rates and relation to estimated iron content *Radiology* 1999; 210: 759-767.
- [44] Bottomley PA, Foster TH, Argersinger RE, Pfeifer LM. A review of normal tissue hydrogen NMR relaxation times and relaxation mechanisms from 1–100 MHz: Dependence on tissue type, NMR frequency, temperature, species, excision, and age. *Medical Physics* 1984; 11: 425-448.
- [45] Orididge RJ, Gorell JM, Deniau JC, *et al.* Assessment of relative brain iron concentration using T2-weighted and T2*-weighted MRI at 3 tesla. *Magn Reson Med* 1994; 32: 335-341.
- [46] Weisskoff RM, Zuo CS, Boxermann JL, *et al.* Microscopic susceptibility variation and transverse relaxation: Theory and experiment. *Magn Reson Med* 1994; 31: 601-610.
- [47] Fujita N. Extravascular contribution of blood oxygenation-level dependent signal changes: a numerical analysis based on a vascular network model. *Magn Reson Med* 2001; 46: 723–734.
- [48] Fujita N, Shinohara M, Tanaka H, *et al.* Quantitative mapping of cerebral deoxyhemoglobin content using MR imaging. *NeuroImage* 2003; 20: 2071-2083.
- [49] Torack RM, Alcalá H, Gado M, Burton R. Correlative assay of computerized cranial tomography CCT, water content and specific gravity in normal and pathological postmortem brain. *J Neuropathol Exp Neurol* 1976; 35: 385-92.
- [50] Chen JC, Hardy PA, Kucharczyk W, *et al.* MR of human postmortem brain tissue: correlative study between T2 and assay of iron and ferritin in Parkinson and Huntington Disease. *American Journal of Radiology* 1993; 14: 275-281.
- [51] Bartzokis G, Sultzer D, Cumming JL, *et al.* *In vivo* evaluation of brain iron in Alzheimer's disease and normal controls using magnetic resonance imaging. *Arch Gen Psychiatry* 2000; 57: 47-53.
- [52] Le Bihan D, Breton E, Lallemand D, *et al.* MR imaging of intravoxel incoherent motions: application to diffusion and perfusion in neurologic disorders. *Radiology* 1986; 161: 401-407.
- [53] Abe K. Early pathological changes in the parkinsonian brain. *J Neurol Neurosurg Psychiatry* 2004; 75: 352-353.
- [54] Yablonsky DA, Haacker EM. Theory of NMR signal behavior in magnetically inhomogeneous tissues: the static dephasing regime. *Magn Reson Med* 1994; 32: 749-763.